Experimental Thermal and Fluid Science 119 (2020) 110211

Contents lists available at ScienceDirect

Experimental Thermal and Fluid Science

journal homepage: www.elsevier.com/locate/etfs

Analysis of reattachment length dynamics in cavities

Paulius Vilkinis*, Nerijus Pedišius

Laboratory of Heat-Equipment Research and Testing, Lithuanian Energy Institute, Breslaujos str. 3, Kaunas LT-44403, Lithuania

ARTICLE INFO

Keywords:
Cavity flow
Reattachment length
Shear layer separation
Recirculation zone dynamics

ABSTRACT

Recirculation zone dynamics in a cavity located in the bottom wall of a water channel with height h = 0.3 mm and width b = 0.9 mm are investigated experimentally and numerically.

A microparticle image velocimetry method and instrumentation are used for the experimental determination of flow velocity distribution and reattachment pattern with Reynolds number from Re_{Dh} = 30–2000, cavity length to depth ratios of L/h_1 = 10 and 16, and channel expansion ratios of H/h = 1.3, 1.5, 2, 3, and 5. Numerical simulation using commercially available Ansys Fluent software is conducted for analysis of the influence of flow regime and cavity dimensions by changing Re_{Dh}, L/h_1, and H/h in the ranges of ($1–10^5$), (8–36) and (1.25–5), respectively.

The experimental and numerical simulation results show that in a laminar flow regime reattachment length increases with increasing Re_{Dh} in the same manner as in flow over a backward-facing step. Re_{h1} and H/h are the main scaling parameters for the reattachment length. However, the results suggest that the transition to a turbulent flow regime occurs earlier due to the small channel spanwise aspect ratio AR = b/h = 3. $Re_{h1} \approx 500$ and $Re_{h1} \approx 2000$ are the critical values that determine the onset of flow transition from a laminar to a turbulent regime and the onset of fully developed turbulent flow, respectively. In addition, it is found that the influence degree of channel expansion ratio depends on whether H/h > 2 or H/h < 2.

1. Introduction

Flow separation phenomenon and recirculating flows are relevant to many practical and fundamental applications. Flow separation usually occurs at abrupt changes in the channel cross-section area or its wall geometry and is caused by an adverse pressure gradient. Flow over a single backward-facing step is the simplest and most examined pattern [1]. However, in many applications, channel expansion due to abrupt steps in a wall is limited by forward-facing step narrowing of the channel cross-section. In such cases, a local cavity forms in the channel wall with flow dynamics similar to the flow dynamics over a single backward-facing step. However, the flow over a cavity shows different behaviours due to confinement of expanded channel length. Cavities are frequently encountered in practical applications including heat transfer surfaces of heat exchangers and heat sinks [2,3], as well as various mixing enhancement [4–6] and biofluidic applications [7,8]. When flow separates from the edge of a backward-facing step, the flow and thermal boundary layer redevelop in the cavity. This redeveloping flow is characterised by enhanced heat transfer processes along the length of the cavity. The length of redeveloping flow depends on the flow regime, cavity type, and the geometric parameters. Knowledge of separated flow dynamics in cavities is crucial to improving heat transfer in cavity-like geometries.

In our previous work [9], flow structure in a transitional-type cavity was investigated dependent on the flow regime when the influence of a forward-facing step is evident for reattachment length. It was shown that a system of periodically detached vortices is formed behind the backward-facing step in a turbulent flow regime and determines the asymptotic value of reattachment length. Large eddy simulation (LES) revealed that the size of the primary vortex behind the backward-facing step is determined by the depth of the cavity, and the primary vortex separates from the edge of the backward-facing step after critical size is reached. From these results it is evident that the behaviour of the recirculation zone in the cavity has an impact on heat transfer processes on the bottom of the cavity because the stagnant recirculation zone in transitional flow regime reduces heat transfer efficiency.

Zhang et al. [10] investigated flows at different cavity length-to-depth (L/h_1) ratios and found that transition from open to transitional-type flow occurs at L/h_1 = 10–12 and change from transitional to closed-type flow occurs at L/h_1 = 14 in supersonic flows. Coleman et al. [11] found that flow structure in a cavity changes at L/h_1 = 5 when principal vortices swap their positions. Leonardi et al. [12]

* Corresponding author.
E-mail addresses: paulius.vilkinis@lei.lt (P. Vilkinis), nerijus.pedisius@lei.lt (N. Pedišius).

https://doi.org/10.1016/j.expthermflusci.2020.110211
Received 28 November 2019; Received in revised form 31 March 2020; Accepted 24 June 2020
Available online 29 June 2020

Nomenclature

AR	spanwise aspect ratio, AR = b/h
b	channel width (m)
D_{ij}	turbulent diffusion production
ε_{ij}	dissipation
F_{ij}	rotation production
H	height of the channel in the cavity cross-section (m), H = (h + h_1)
h	height of the channel (m)
h_1	cavity depth (m)
L	cavity length (m)
P_{ij}	a term for stress production
RANS	Reynolds-averaged Navier-Stokes equations
Re	Reynolds number
Re_{Dh}	channel Reynolds number
Re_{h1}	cavity Reynolds number
ρ	density, kg/m^3
RSM-BSL	Reynolds-stress baseline model
x_r	reattachment length (m)
Φ_{ij}	pressure strain

observed that for $L/h_1 > 7$, the strength and size of the main recirculation zone no longer depend on L/h_1. Palharini et al. [13] showed that in certain conditions closed-type cavity flow can occur when $L/h_1 = 5$. Nevertheless, the reported results on cavity flow do not agree. To the best of our knowledge, no reattachment length analysis on geometric cavity parameters was performed.

A more detailed analysis of reattachment length was performed on the flows over various backward-facing steps. Studies of flows over backward-facing steps show that reattachment length depends on flow regime in the channel and three reattachment length patterns can be distinguished [14–16]. These patterns have been confirmed many times in different channels and obstacle geometries. In a laminar flow regime, reattachment length increases linearly with Re number [16–20] until it becomes unstable in a transitional flow regime [16]. Studies have shown that reattachment length abruptly decreases after transition to a transitional flow regime [14,19] until a turbulent flow regime is reached; reattachment length saturates and becomes nearly independent of Re. As reported in Chen et al. [1], for a fully developed turbulent flow regime, reattachment length falls in a saturated range of 6–8 step (or obstacle) heights, regardless of other geometric parameters.

Abrupt channel expansion causes an adverse pressure gradient in the cavity, which leads to flow separation. The effect of channel expansion ratio on flow structure has been widely investigated on flows over backward-facing steps [1,19,21]. It was shown that vortex intensity [17], as well as flow complexity and formation of additional recirculating zones behind backward-facing steps [12], depend on channel expansion ratio. Several authors investigated dependence of reattachment length dynamics on channel expansion ratio [16,22,23]. In research by Nadge and Govardhan [22], it is reported that in a turbulent flow regime reattachment length increases linearly until $H/h = 1.8$ is reached, and remains constant at higher values. Biswas et al. [18] showed that reattachment length increases with the expansion ratio in a laminar flow regime in the range of $H/h = 2–3$. However, the mechanism changing separated flow dynamics at different channel expansion ratios is still unclear. The problem becomes even more complicated when a forward-facing step is present, influencing recirculating flow dynamics.

In certain applications [23,24], it is critical to know the length of the recirculation zone. Heat transfer intensity is enhanced at the location where the shear layer reattaches to the bottom of the cavity [25–28]. The shear mixing layer length can also be evaluated [4]. Gong et al. [23] suggested an equation for recirculation zone length for flow over a backward-facing step, with an error < 2.5% for 40 < Re < 200:

$$\frac{x_r}{(H/h-1)h} = 0.112Re - 0.27, \text{ for} 2.6 \le H/h \le 200 \quad (1)$$

Tihon et al. [16] proposed a formula for the reattachment length in the form

$$H/h\left(\frac{x_r}{h_1}\right) = 0.3Re_h^{0.375} \quad (2)$$

with an error < 7% for $1.25 \le H/h \le 5$ and $Re_h < 200$.

Cantwell et al. [20] presented linear dependence on Re for recirculation zone length in an axisymmetric circular pipe in the form

$$\frac{x_r}{h_1} = 0.0876Re \quad (3)$$

As observed from the literature review, dynamics of recirculation flow, caused by abrupt channel expansion (backward-facing step, obstacle, or a cavity in the channel), depend on geometric parameters and flow regime. However, there is a lack of generalisation of parameters determining reattachment length dynamics over a wide range of Re and geometric parameters, especially in cavities.

In this study, a cavity with arched steps is used. Usually, experiments and numerical studies are conducted for vertical, 90 degrees, steps for flows over a backward-facing step [15–17,19], and cavities [12,29,30]. Flows over different step geometries have attracted less research attention. Several studies investigated flow over inclined [31–33] and rounded [34] backward-facing steps. However, to the best of our knowledge, reattachment length dynamics in cavities with rounded steps have never been investigated.

The purpose of this study is to generalise reattachment length dynamics in cavities depending on flow regime and geometric parameters, relating them to fundamental fluid mechanics patterns. In this study, we continue our investigation of reattachment length dynamics in cavities depending on geometric parameters of the cavity and flow regime. Experimentally measured and simulated values of the relative recirculation zone length in cavities are presented over a wider range of Re ($1 \le Re_{Dh} \le 10^5$), relative cavity length ($6 \le L/h_1 \le 36$), and channel expansion ratio ($1.25 \le H/h \le 5$). Hence, the influence of the forward-facing step on reattachment length dynamics in cavities is

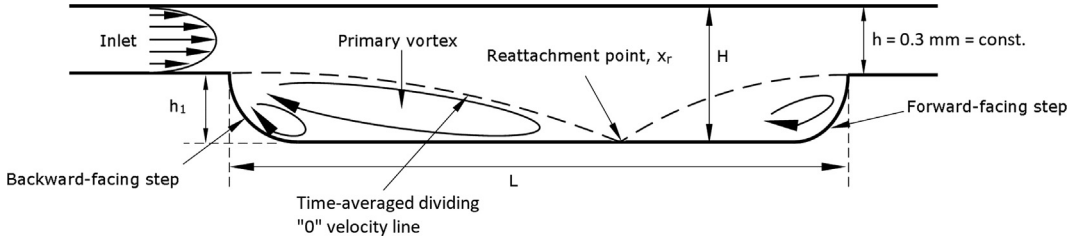

Fig. 1. General scheme of the cavity.

explained. In addition, the influence of channel expansion ratio is generalised by linking to the distribution of an adverse pressure gradient and patterns of stream spreading.

We organize this paper as follows. In Section 2 we introduce experimental set-up and physical object as well as the numerical method used for simulations. Experimentally measured and simulated values of reattachment length over cavities with different geometrical parameters and extensive discussions of obtained results are presented in Section 3. Conclusions are presented in Section 4.

2. Materials and methods

In this study, experimental and numerical methods were employed. Experimental measurements were performed for $Re_{Dh} \leq 2000$. Higher Re_{Dh} values could not be reached due to system limitations. Numerical simulation was applied to reach Re_{Dh} values up to $Re_{Dh} = 10^5$.

2.1. Experimental facility and instrumentation

Experiments were performed in the cavity presented in Fig. 1. The channels have rectangular cross-sections with height h = 0.3 mm and width b = 0.9 mm, with a tolerance of 0.01 mm. The spanwise aspect ratio is b/h = 3, and reattachment length analysis corresponds to three-dimensional channel geometry. One sidewall of the channels contains a transitional or closed-type cavity with depths (h_1) of 0.09, 0.15, 0.6, and 1.2 mm with a tolerance of 0.02 mm and roughness of 0.001–0.005 mm. Cavities are of the same shape as in our previous work [9], but with different dimensions. Cavities with length-to-depth ratios of $L/h_1 = 10$ and $L/h_1 = 16$ and channel expansion ratios of H/h = 1.3, 1.5, 2, 3, and 5 were investigated.

A micro-particle image velocimetry (μPIV) system was used for flow velocity distribution measurements. The location of the shear layer reattachment was determined according to minimum velocity along the cavity bottom where reattaching flow splits into upstream and downstream flows.

Experimental measurements were performed at $Re_{Dh} \leq 2000$. Higher Re_{Dh} values could not be reached due to limited set-up capabilities. Water was used as a working fluid. During measurements, water temperature was maintained at 22 ± 1 °C. Fluorescent 1 μm diameter tracer particles (Invitrogen, Waltham, MA) with a specific gravity of 1.05 and excitation and emission wavelengths of 535 nm and 575 nm, respectively, were introduced into the water flow. The water flow was generated using a programmable syringe pump (WPI AL400) and ensuring the flow rate up to 114.5 ml/min. The μPIV system consisted of a Nd:YAG type laser (Dantec Dynamics), the laser control unit LPU 450 (Dantec Dynamics) and the 2048 × 2048 pixel FlowSense EO CCD camera (Dantec Dynamics) coupled with Leica DM ILM microscope (Leica Microsystems) was used. DynamicStudio (Dantec Dynamics) software was employed for devices control and images analysis. The image pairs of tracer particles were captured at 15 Hz frequency with the time interval in the image frames varied from 5×10^{-3} s to 1×10^{-5} s depending on the flow rate. Time-averaged velocity data were obtained by averaging flow images for at least 10 s of flow. An adaptive correlation algorithm was applied for image processing. A spatial resolution of 20.6 μm × 20.6 μm and depth of correlation of 42.4 μm were achieved.

2.2. Numerical simulation

Commercially available Ansys Fluent software with the Reynolds-stress – Baseline turbulence model (RSM-BSL) was used for two-dimensional numerical simulation at Re_{Dh} values up to $Re_{Dh} = 10^5$ in the range of $6 \leq L/h_1 \leq 36$, and $1.25 < H/h < 5$. The governing transport equation for Reynolds stresses, $\rho \overline{u_i' u_j'}$, is:

$$\frac{\partial}{\partial t}(\rho \overline{u_i' u_j'}) + \frac{\partial}{\partial x_k}(\rho \bar{u}_k \overline{u_i' u_j'}) = P_{ij} + F_{ij} + D_{ij}^T + \Phi_{ij} - \varepsilon_{ij} \quad (4)$$

where P_{ij} is the stress production, F_{ij} is the rotation production, D_{ij}^T is the turbulent diffusion, Φ_{ij} is the pressure strain, and ε_{ij} is the dissipation. The choice of the RSM-BSL model is based on its suitability to capture complex and secondary flows, and its ability to precisely capture flow separation and reattachment.

Grid independence was ensured by computing several different grid levels and monitoring the location of the shear layer reattachment. A grid independence study was performed with an increasing number of cells, thereby decreasing cell size. Four relative grid sizes with respect to cavity height were chosen. Upon decreasing relative cell size from 0.6 to 0.05, reattachment length increased by 8.6%. Further decreasing relative cell size to 0.006, reattachment length decreased 0.5% and remained constant with further decrease of cell size to 0.0003.

Hence, the ratios of minimum and maximum cell height to the height of the cavity were chosen as 0.0015 and 0.006, respectively. The boundary layer was resolved with an inflation layer of 15 cells to assure that y^+ was < 1. The SIMPLEC solution algorithm, together with second-order upwind discretisation schemes were applied in these simulations. As reported in our previous work [9], numerical simulation results using RSM-BSL are in good agreement with experimental results in the laminar flow regime and with the trend of reattachment length dynamics in the turbulent flow regime.

3. Results and discussion

In this section the dependence of relative reattachment length on the channel flow regime, cavity-type, and relative channel expansion is analysed following the function:

$$x_r/h_1 = f(Re_{Dh}, Re_{h1}, L/h_1, \frac{H}{h}) \quad (5)$$

where Re_{Dh} and Re_{h1} are the Re numbers based on channel hydraulic

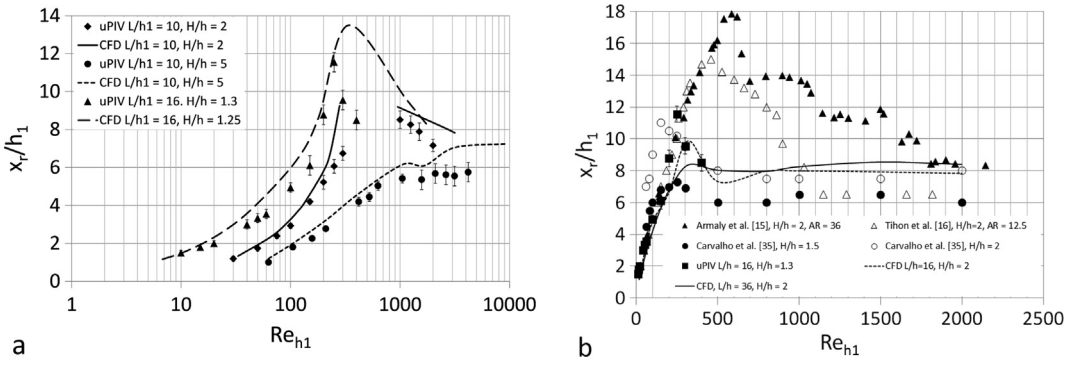

Fig. 2. (a) comparison of experimentally measured and simulated reattachment length values, (b) dependence of reattachment length on Re_{h1} for different cases of flow over backward-facing step and obstacles.

diameter and cavity depth respectively, L/h_1 is the relative cavity length defining the cavity type, and H/h is the ratio of channel heights at the cavity cross-section and before a cavity.

3.1. Validation of the results

Fig. 2a demonstrates that simulated reattachment length values fit the experimental data in the laminar flow regime. However, it is clear that employed RSM-BSL model struggles to predict transition for laminar to turbulent flow regime. Discrepancies occur while approaching the transitional flow regime; simulated results provide higher reattachment length values and transition to the transitional flow regime occurs at higher Re numbers. However, the trends of reattachment length values remain the same. These discrepancies were determined by the two-dimensional simulations and an oversimplification of RANS simulations when averaging recirculating flow.

Fig. 2b presents a comparison of reattachment length values in flows over different backward-facing steps geometries and our cavities. A three-dimensionality effect on reattachment length dynamics is observed in this comparison. Comparing the data provided by Armaly et al. [15] and Tihon et al. [16], the influence of the channel aspect ratio is evident. Measured reattachment length values are lower and transition to the transitional flow regime occurs more abruptly in the lower channel aspect ratio case presented by Tihon et al. Lower reattachment length values at the transition to transitional flow regime are observed in our study. In our study, the channel aspect ratio is equal to 3, therefore flow in the channel is heavily three-dimensional. Additionally, the steps of the cavities are rounded, decreasing reattachment length, as shown in research by Bravo et al. [34]. Measured and simulated reattachment length values in our cavity are lower than in flows over a conventional backward-facing step. Our data also correlates well with measurements of reattachment length over the two-dimensional fence by Carvalho et al. [35] with different channel blockade ratios. It is observed that both channel aspect ratio and geometry have a significant influence on reattachment length dynamics.

3.2. Reattachment length dependence on flow regime and cavity type

As observed in the experimental and numerical simulation results presented in Figs. 3, 4, and 5, reattachment length variation trends are strongly determined by the flow regime. For laminar flow, a single main vortex forms behind the backward-facing wall of the cavity that increases in length with increasing Re_{Dh} until a transition to the turbulent flow regime or significant influence of the forward-facing step occurs.

The latter phenomenon is observed in the transitional-type cavity when its relative length is $L/h_1 = 8–12$ (Figs. 3 and 4). In such a case, the forward-facing cavity wall lifts the reattaching shear layer from the cavity bottom, and stagnant closed recirculating flow occurs along the entire cavity length. The marked lifting of the reattaching shear layer becomes noticeable when the reattachment point reaches approximately the middle of the cavity. The inner structure of flow in the transitional-type cavity was reported in our previous study [9]. Reattachment to the cavity bottom occurs again in the cavity when fundamental changes in the internal structure of vortices behind the backward cavity wall induce the transition to a turbulent flow regime. The transition to a transitional flow regime occurs at different Re_{Dh} values depending on the relative length of the cavity. For $L/h_1 = 8$, 10, and 12 the attachment to the bottom wall of the cavity is observed until $Re_{Dh} = 170$, 280, and 300, respectively. The reappearance of shear layer attachment occurs at higher Re_{Dh} values for cavities with shorter relative length; $Re_{Dh} = 2500$, 950, and 830 for $L/h_1 = 8$, 10, and 12, respectively. The Re_{Dh} interval in which shear layer attachment is absent narrows as relative cavity length increases. This is explained by the weaker influence of the forward wall of the cavity as cavity length increases.

Experimental and numerical results of relative reattachment length (x_r/h_1) for a wide range of Re_{Dh} and cavity length-to-depth ratios ($4 \leq L/h_1 \leq 36$) are presented in Fig. 4. Other cavity parameters (cavity depth h_1, expansion ratio H/h) are kept constant. In this case, all three types of cavities (open, transitional, and closed-type) are observed. When the relative length of the cavity is less than $L/h_1 = 6$, the reattachment phenomenon in the cavity does not occur and the cavity is an open-type, which is beyond the scope of this study. The separated shear layer bridges over the cavity without penetrating deep into the cavity. Reattachment to the bottom wall of the cavity is observed when $L/h_1 = 6$ is reached. However, the shear layer attaches to the bottom wall only at low values of $Re_{Dh} \leq 85$. Exceeding this value, flow structure in the cavity becomes open-type in the remaining Re_{Dh} range.

As observed in Fig. 4, when $L/h_1 \geq 14$ is reached, the cavity gradually becomes a closed-type and shear layer reattachment to the bottom of the cavity occurs in the entire investigated Re_{Dh} range. However, the peak value of relative reattachment length decreases as relative cavity length increases to $L/h_1 = 18$. As the cavity elongates from $L/h_1 = 14$ to $L/h_1 = 16$, x_r/h_1 decreases 14% from 11.5 to 9.85 step heights. However, as cavity relative length changes from $L/h_1 = 16$ to $L/h_1 = 18$, x_r/h_1 decreases 4.5% from 8.75 to 8.35 step heights. Apparently, x_r/h_1 approaches an asymptotic value as relative cavity length increases, and the influence of the forward-facing wall of the cavity is negligible. Flow structure in the cavity becomes similar to the flow over a backward-facing step. In the cases of transitional and closed-type cavities, in a fully developed turbulent flow regime, relative recirculation zone length approaches an asymptotic value independent of the length of the cavity.

In a closed-type cavity (Fig. 5) the peak value of relative reattachment length decreases as channel expansion ratio increases. In this case, with different H/h values, inlet channel height, h, is kept constant and cavity depth, h_1 (and thereby H), is changing. Higher channel expansion ratio leads to faster growth of the separated shear layer, forcing the shear layer to attach to the bottom wall of the cavity at a shorter distance from the backward-facing wall. The peak value of recirculation zone length occurs at higher Re_{Dh} as channel expansion ratio decreases. This shift indicates that the transition to a turbulent flow regime occurs at higher Re_{Dh} values as channel expansion ratio decreases.

In a closed-type cavity (Fig. 5), there is a clear view of the reattachment length layering according to the cavity geometric parameters in the laminar flow regime. However, there is less layering in a transitional-type cavity (Fig. 3). For $H/h = 5$ in transitional and closed-type cavities, reattachment length values are similar over the entire range of investigated Re_{Dh}. In a transitional-type cavity (Fig. 3), shear layer attachment to the bottom wall of the cavity persists over the entire Re_{Dh} range, while absence of shear layer attachment in a

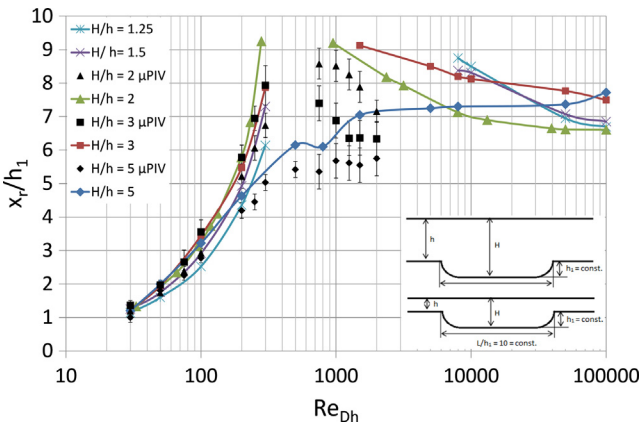

Fig. 3. Dependence of relative reattachment length on Re_{Dh} for different H/h values in the transitional-type cavity ($L/h_1 = 10$); curves represent numerical simulation results, points with error bars represent experimentally measured results.

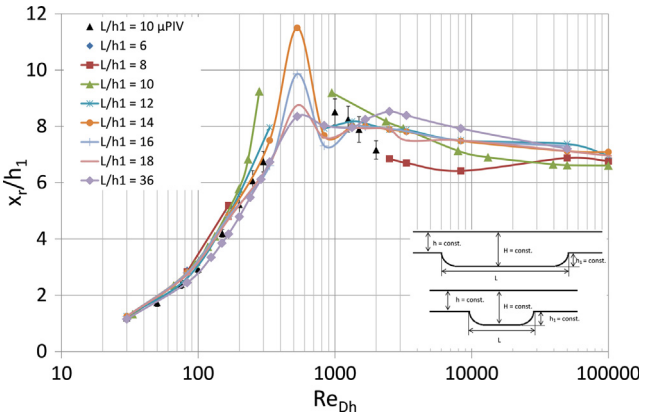

Fig. 4. Dependence of relative reattachment length on Re_{Dh} for different relative lengths of cavities at H/h = 2; curves represent numerical simulation results, points with error bars represent experimentally measured results.

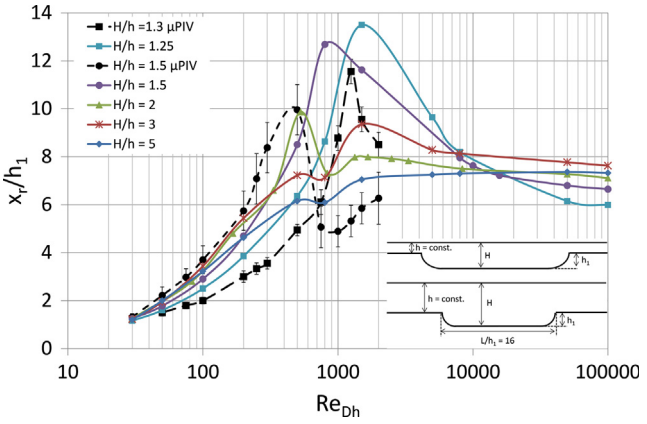

Fig. 5. Dependence of relative recirculation zone length on Re_{Dh} for different H/h values in a closed-type cavity (L/h_1 = 16); points with error bars represent experimentally measured results.

transitional flow regime is typical for a transitional-type cavity [9].

The results show that to generalise the reattachment length dynamics, parameters estimating the cavity geometry must be introduced. One parameter must be the cavity depth, which in turbulent mode limits the size of the intermittent main vortices and determines the stability of x_r/h_1 independently of Re_{Dh}. The H/h parameter is also critical.

3.3. Reattachment length dependence on cavity depth (h_1) and channel expansion ratio (H/h)

Considering that abrupt channel expansion caused by the cavity is the source of flow separation and forms the recirculation circuit, separated shear layer reattachment length must be dependent on the depth of the cavity (h_1). The relationship between x_r and h_1 is already introduced as the relative reattachment length (x_r/h_1). However, h_1 can be used as a parameter in the evaluation of Reynolds number. Re_{h1} becomes a parameter determining reattachment length dependence on both the flow regime and depth of the cavity. Re_{h1} and Re_{Dh} are both widely used in the investigation of reattachment length dynamics behind a backward-facing step [1,16,18].

Dependence of relative reattachment length values on Re_{h1} in a closed-type cavity is presented in Fig. 6. In a transitional-type cavity, patterns are the same, but with no reattachment at certain Re_{h1} values (Figs. 3 and 4). Therefore, for further analysis, data from closed-type cavities are presented. It is observed that peak relative recirculation zone length values occur at the same Re_{h1} when H/h ≤ 2. At higher values of H/h, peak values of x_r/h_1 are slightly shifted toward higher Re_{h1} values. In addition, as H/h value increases, x_r/h_1 decreases at the same Re_{h1} in a laminar flow regime. The reverse is observed in the turbulent flow regime; x_r/h_1 increases as H/h increases at the same Re_{h1}.

Fig. 7 presents dependence of relative reattachment length on channel expansion ratio for different Re_{Dh} values. Generally, reattachment length increases as channel expansion ratio increases from 1.25 to 2. In a laminar flow regime, peak values of x_r/h_1 are reached when H/h = 2. In a transitional flow regime, peak values occur in the range of 1.5 ≤ H/h ≤ 2. In a turbulent flow regime, the peak value is reached when H/h = 3. The fastest-growing rates of x_r/h_1 are observed in laminar (Re_{Dh} = 200) and transitional flow regimes; the slowest rate is at low Re_{Dh} values and in a turbulent flow regime. Increasing H/h further, relative reattachment length decreases. The rate of decline is fastest in the transitional flow regime and insignificant in laminar and turbulent flow regimes.

From patterns presented in Fig. 6, it is observed that in a laminar flow regime reattachment length values (x_r/h_1 = f(Re_{h1})) are consistently layered according to channel expansion ratio (H/h). It was reported by Tihon et al. [16] that parameter H/h can be used for reattachment length scaling. However, from the physical point of view, it is more expedient to relate channel expansion ratio with expansion of the mixing layer formed due to the interaction of the separated shear layer with the recirculating flow behind the backward-facing wall. It is known that the growth rate of the separated shear (mixing) layer is determined by the transversal velocity pulsation component and can be estimated as

$$d = \frac{v_1 - v_2}{v_1 + v_2} x \tag{6}$$

where v_1 is the mean channel flow velocity at the inlet to the cavity, v_2 is the mean flow velocity in the cavity cross-section, and x is the distance from the inlet to the cavity.

In our case, the asymmetric spreading of flow enters the cavity. v_2 is chosen as the mean velocity in the cavity, which decreases h/H times compared to the mean velocity in the channel before entering the cavity. The dependence of the separated shear layer spreading rate is presented in Fig. 8.

As observed in Fig. 6, distinct peaks of reattachment length at the transition from laminar to turbulent flow regime are observed only when H/h ≤ 2. Further increasing Re_{Dh}, relative reattachment length decreases and approaches an asymptotic value in a fully developed turbulent flow regime. However, for H/h > (2–3), smooth reattachment length growth without a well-defined peak is observed. It is apparent that the adverse pressure gradient in the cavity increases as the channel expansion ratio increases (dp/dx > 0). The adverse pressure

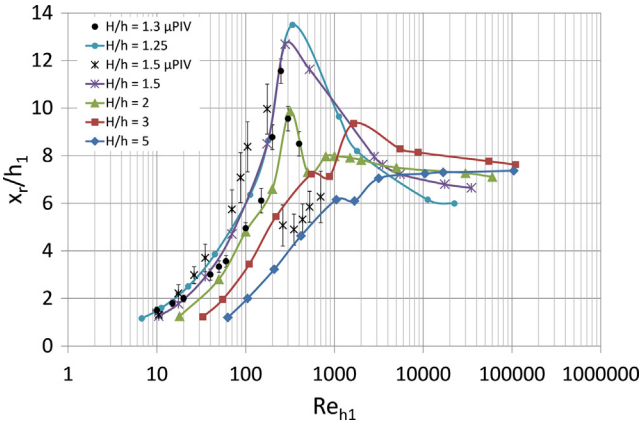

Fig. 6. Dependence of relative recirculation zone length on Re_{h1} for different H/h values in a closed-type cavity (L/h_1 = 16).

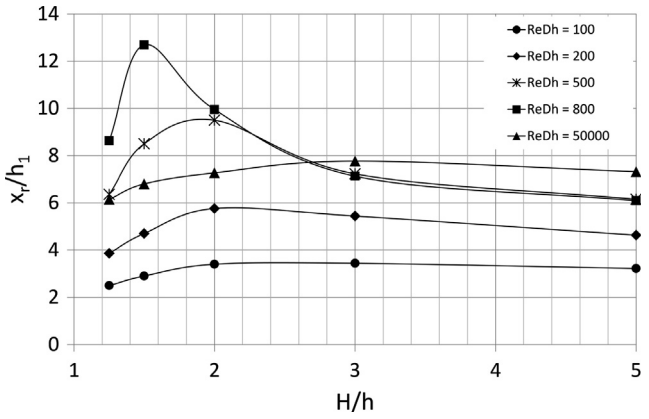

Fig. 7. Dependence of relative recirculation zone length on H/h at different Re_{Dh} values in a closed-type cavity ($L/h_1 = 16$).

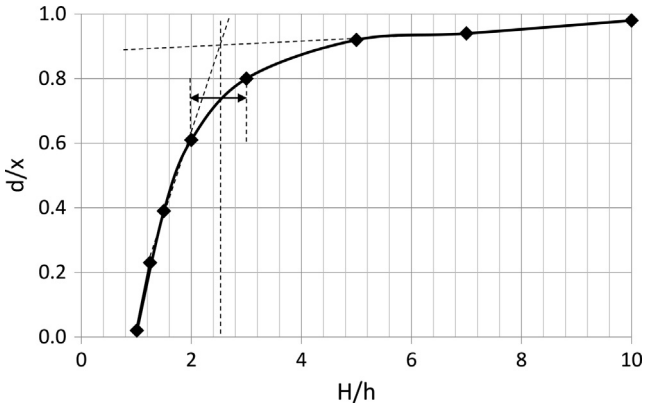

Fig. 8. Dependence of spreading rate of the separated shear layer in the cavity on channel expansion ratio.

gradient forces the shear layer to reattach to the bottom wall of the cavity at a shorter distance. Whereas, the separated shear layer spreading rate increases as the channel expansion ratio increases. For this reason, shear layer reattachment occurs at a shorter distance and relative reattachment length shortens as H/h increases. The influence of the adverse pressure gradient and shear layer spreading rate becomes dominant in the cavity as it changes reattachment length pattern in a transitional-type cavity (Fig. 3, H/h = 5). The recirculation zone is stabilised by the high adverse pressure gradient and the laminar flow regime persists up to higher Re_{h1} values (Fig. 6). In addition, the influence of the forward-facing step becomes insignificant at high channel expansion ratios.

The turning point in Fig. 8 corresponds to the H/h value at which the mixing layer spreading rate and the dynamics of recirculation zone length change their patterns in the cavity. The turning point is in the range of H/h ≈ 2–3. As observed in Figs. 4–6, relative reattachment length dependence on Re can be separated into two groups, H/h < 2 and H/h > 2. For H/h < 2, defined peaks and higher maximum relative reattachment length are observed than for H/h > 2. When H/h > 2 (especially when H/h = 5), relative recirculation zone length monotonically increases until the asymptotic value in a turbulent flow regime is approached.

3.4. Reattachment length scaling

Parameter $(H/h)(x_r/h_1)$ versus Re_{h1} for scaling of reattachment length was first introduced by Tihon et al. for laminar flow over a single backward-facing step. Dependence of $(H/h)(x_r/h_1)$ on Re_{h1} for flow over cavities is presented in Fig. 9. As observed, this parameter performs well for fitting data in the laminar flow regime. Peak values still occur at the same Re_{h1} when H/h ≤ 2. However, in the turbulent flow regime $(H/h)(x_r/h_1)$ is directly proportional to the channel expansion ratio (H/h) component. Nevertheless, from the data presented in Fig. 6, we see that parameter x_r/h_1 versus Re_{h1} works satisfactorily for fitting data points in a turbulent flow regime.

Fig. 10 presents the dependence of reattachment length on Re_{h1} in transitional and closed-type cavities. Reattachment length values in a laminar flow regime are depicted on the left side of the graph. The data can be fitted to

$$\left(\frac{H}{h}\right)\left(\frac{x_r}{h_1}\right) = 0.35Re_{h1}^{0.7} \tag{7}$$

This relationship is strong for low Re_{h1} values; scattering increases with Re_{h1}. The uncertainty is 8% when $0 < Re_{h1} < 100$, 10% when $100 < Re_{h1} < 200$, and 16% when $200 < Re_{h1} < 350$. For comparison, the relation for backward-facing step flow estimated by Tihon et al. [16] is valid for $Re < 200$ with an error of < 7%. The different coefficients used are determined by differences in geometries, and the presence of a forward-facing step for cavity flow.

On the right side of Fig. 10, the dependence of relative reattachment length on Re_{h1} for a turbulent flow regime is presented. Because the reattachment length in the turbulent flow regime depends only on Reynolds number, cavity geometry does not influence the structure of the flow. The relation can be written as

$$\left(\frac{x_r}{h_1}\right) = 7 + 50Re_{h1}^{-0.55} \tag{8}$$

This relation becomes stronger as Re_{h1} increases because in a fully developed turbulent flow regime, relative recirculation zone length approaches its asymptotic value, which is in the range of 6 to 8 step heights. The uncertainty is approximately 20% when $500 < Re_{h1} < 10^4$, and 12% when $10^4 < Re_{h1} < 10^5$. The recirculation zone enters the system of vortices after transition to a turbulent flow regime [9]. The mean location of vortices attachment no longer depends on Re_{h1} and remains constant.

4. Conclusions

In this study, dynamics of reattachment length in transitional and closed-type cavities depending on geometric parameters under laminar, transitional, and turbulent flow regimes were investigated using experimental and numerical approaches. Flow in the investigated cavity is three-dimensional and the channel aspect ratio b/h = 3. In laminar and

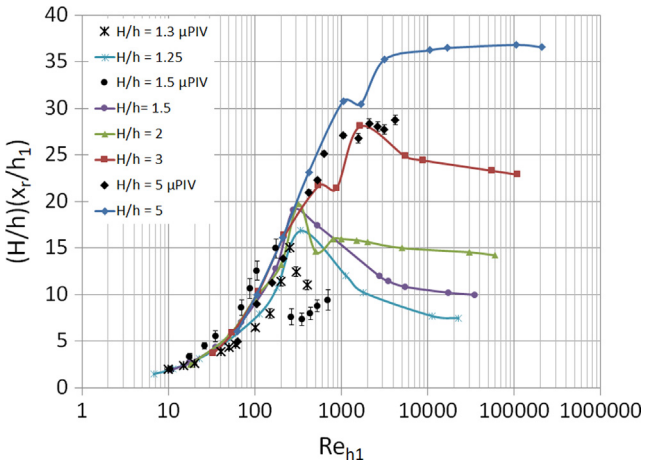

Fig. 9. Dependence of relative reattachment length multiplied by channel expansion ratio on Re_{h1} for different H/h values in a closed-type cavity ($L/h_1 = 16$).

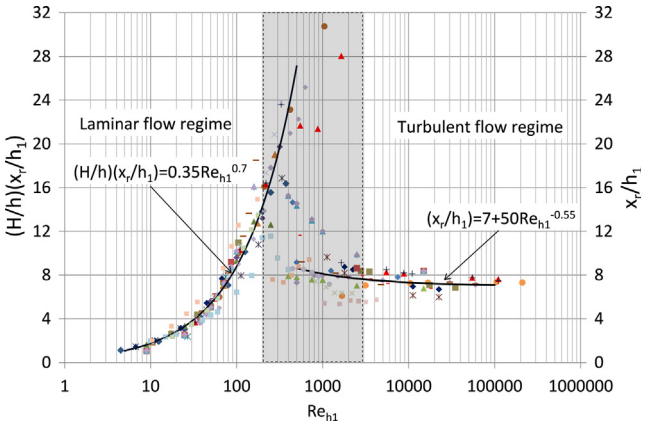

Fig. 10. Relation of recirculation zone length in laminar and turbulent flow regimes.

turbulent flow regimes, reattachment length dynamics correlate with the flow over a backward-facing step. However, discrepancies were revealed in the transitional flow regime; flow in the cavity is mostly influenced by channel expansion ratio and cavity type.

With increasing relative cavity length (L/h_1), transitional-type cavity flow occurs at $L/h_1 = 6$ and changes to a closed-type cavity at $L/h_1 = 14$. Peak relative reattachment length is also reached at $L/h_1 = 14$. Increasing relative cavity length further, the peak value of x_r/h_1 decreases until $L/h_1 = 18$ and becomes nearly constant at higher L/h_1 values because the influence of the forward-facing step becomes insignificant. It is apparent that the forward-facing step lifts the re-attaching shear layer from the bottom of the cavity and consequently increases reattachment length.

Channel expansion ratio H/h determines the expansion of the separated shear layer and adverse pressure gradient in the cavity. For low channel expansion ratios ($H/h \leq 2$), reattachment length reaches higher values with defined peaks at the transition from a laminar to a transitional flow regime. For high channel expansion ratios ($H/h > 2$), an adverse pressure gradient forces the separated shear layer to re-attach at a shorter distance from the backward-facing step of the cavity. At $H/h = 5$, a transition from laminar to turbulent flow regime occurs smoothly without defined reattachment length peaks.

Recirculation zone length in a laminar flow regime can be estimated as $(x_r/h_1)\left(\frac{H}{h}\right) = 0.35Re_{h1}^{0.7}$. This relation persists until the transition to a turbulent flow regime is reached. After the transition to a turbulent flow regime, recirculation zone length approaches its asymptotic value and can be estimated as $(x_r/h_1) = 7 + 50Re_{h1}^{-0.55}$.

Declaration of Competing Interest

The authors report no conflict of interest.

References

[1] L. Chen, K. Asai, T. Nonomura, G. Xi, T. Liu, A review of Backward-Facing Step (BFS) flow mechanisms, heat transfer and control, Therm. Sci. Eng. Prog. 6 (2018) 194–216, https://doi.org/10.1016/j.tsep.2018.04.004.

[2] C. Herman, E. Kang, Heat transfer enhancement in a grooved channel with curved vanes, Int. J. Heat Mass Transf. 45 (2002) 3741–3757, https://doi.org/10.1016/S0017-9310(02)00092-3.

[3] Y. Zhai, G. Xia, Z. Chen, Z. Li, Micro-PIV study of flow and the formation of vortex in micro heat sinks with cavities and ribs, Int. J. Heat Mass Transf. 98 (2016) 380–389, https://doi.org/10.1016/j.ijheatmasstransfer.2016.03.044.

[4] W. Huang, Supersonic mixing augmentation mechanism induced by a wall-mounted cavity configuration, J. Zhejiang Univ. Sci. A. 17 (2016) 45–53, https://doi.org/10.1631/jzus.A1500244.

[5] V. Nenmeni, K. Yu, Cavity-induced mixing enhancement in confined supersonic flows, in: 40th AIAA Aerosp. Sci. Meet. Exhib., American Institute of Aeronautics and Astronautics, Reston, Virigina, 2002. https://doi.org/10.2514/6.2002-1010.

[6] K. Ward, Z.H. Fan, Mixing in microfluidic devices and enhancement methods, J. Micromech. Microeng. 25 (2015) 094001, , https://doi.org/10.1088/0960-1317/25/9/094001.

[7] M. Khabiry, B.G. Chung, M.J. Hancock, H.C. Soundararajan, Y. Du, D. Cropek, W.G. Lee, A. Khademhosseini, Cell Docking in Double Grooves in a Microfluidic Channel, Small 5 (2009) 1186–1194, https://doi.org/10.1002/smll.200801644.

[8] Y.-H. Jang, C.H. Kwon, S.B. Kim, Š. Selimović, W.Y. Sim, H. Bae, A. Khademhosseini, Deep wells integrated with microfluidic valves for stable docking and storage of cells, Biotechnol. J. 6 (2011) 156–164, https://doi.org/10.1002/biot.201000394.

[9] P. Vilkinis, N. Pedišius, M. Valantinavičius, Investigation of Flow Dynamics Over Transitional-Type Microcavity, J. Fluids Eng. 140 (2018) 1–7, https://doi.org/10.1115/1.4039159.

[10] F. Zhang, Y. Bian, Y. Liu, J. Pan, Y. Yang, H. Arima, Experimental and numerical analysis of heat transfer enhancement and flow characteristics in grooved channel for pulsatile flow, Int. J. Heat Mass Transf. 141 (2019) 1168–1180, https://doi.org/10.1016/j.ijheatmasstransfer.2019.06.100.

[11] S.E. Coleman, V.I. Nikora, S.R. McLean, E. Schlicke, Spatially Averaged Turbulent Flow over Square Ribs, J. Eng. Mech. 133 (2007) 194–204, https://doi.org/10.1061/(ASCE)0733-9399(2007)133:2(194).

[12] S. Leonardi, P. Orlandi, R.J. Smalley, L. Djenidi, R.A. Antonia, Direct numerical simulations of turbulent channel flow with transverse square bars on one wall, J. Fluid Mech. 491 (2003) 229–238, https://doi.org/10.1017/S0022112003005500.

[13] R.C. Palharini, T.J. Scanlon, C. White, Chemically reacting hypersonic flows over 3D cavities: Flowfield structure characterisation, Comput. Fluids. 165 (2018) 173–187, https://doi.org/10.1016/j.compfluid.2018.01.029.

[14] L.H. Back, E.J. Roschke, Shear-Layer Flow Regimes and Wave Instabilities and Reattachment Lengths Downstream of an Abrupt Circular Channel Expansion, J. Appl. Mech. 39 (1972) 677–681, https://doi.org/10.1115/1.3422772.

[15] B.F. Armaly, F. Durst, J.C.F. Pereira, B. Schönung, Experimental and theoretical investigation of backward-facing step flow, J. Fluid Mech. 127 (1983) 473, https://doi.org/10.1017/S0022112083002839.

[16] J. Tihon, V. Pěnkavová, J. Havlica, M. Šimčík, The transitional backward-facing step flow in a water channel with variable expansion geometry, Exp. Therm. Fluid Sci. 40 (2012) 112–125, https://doi.org/10.1016/j.expthermflusci.2012.02.006.

[17] A. Goharzadeh, P. Rodgers, Experimental Measurement of Laminar Axisymmetric Flow Through Confined Annular Geometries With Sudden Inward Expansion, J. Fluids Eng. 131 (2009) 124501, , https://doi.org/10.1115/1.4000482.

[18] G. Biswas, M. Breuer, F. Durst, Backward-Facing Step Flows for Various Expansion Ratios at Low and Moderate Reynolds Numbers, J. Fluids Eng. 126 (2004) 362–374, https://doi.org/10.1115/1.1760532.

[19] I.A. Stogiannis, A.D. Passos, A.A. Mouza, S.V. Paras, V. Pěnkavová, J. Tihon, Flow investigation in a microchannel with a flow disturbing rib, Chem. Eng. Sci. 119 (2014) 65–76, https://doi.org/10.1016/j.ces.2014.07.055.

[20] C.D. Cantwell, D. Barkley, H.M. Blackburn, Transient growth analysis of flow through a sudden expansion in a circular pipe, Phys. Fluids. 22 (2010) 034101, , https://doi.org/10.1063/1.3313931.

[21] C.-H. Cheng, C.-L. Chen, Buoyancy-induced periodic flow and heat transfer in lid-driven cavities with different cross-sectional shapes, Int. Commun. Heat Mass Transf. 32 (2005) 483–490, https://doi.org/10.1016/j.icheatmasstransfer.2004.10.001.

[22] P.M. Nadge, R.N. Govardhan, High Reynolds number flow over a backward-facing step: structure of the mean separation bubble, Exp. Fluids. 55 (2014) 1657, https://doi.org/10.1007/s00348-013-1657-5.

[23] S.C. Gong, R.G. Liu, F.C. Chou, A.S.T. Chiang, Experiment and simulation of the recirculation flow in a CVD reactor for monolithic materials, Exp. Therm. Fluid Sci. 12 (1996) 45–51, https://doi.org/10.1016/0894-1777(95)00067-4.

[24] A. Mariotti, G. Buresti, M.V. Salvetti, Use of multiple local recirculations to increase the efficiency in diffusers, Eur. J. Mech. - B/Fluids. 50 (2015) 27–37, https://doi.org/10.1016/j.euromechflu.2014.11.004.

[25] T. Kořínek, T. Tisovský, Study of heat transfer in backward-facing step flow using partially-averaged Navier-Stokes (PANS) turbulence modeling method, in: Top. Probl. Fluid Mech. 2019, Institute of Thermomechanics, AS CR, v.v.i., 2019: pp. 123–130. https://doi.org/10.14311/TPFM.2019.018.

[26] F. Selimefendigil, H.F. Öztop, Forced convection and thermal predictions of pulsating nanofluid flow over a backward facing step with a corrugated bottom wall, Int. J. Heat Mass Transf. 110 (2017) 231–247, https://doi.org/10.1016/j.ijheatmasstransfer.2017.03.010.

[27] F. Selimefendigil, H.F. Öztop, Influence of inclination angle of magnetic field on mixed convection of nanofluid flow over a backward facing step and entropy generation, Adv. Powder Technol. 26 (2015) 1663–1675, https://doi.org/10.1016/j.apt.2015.10.002.

[28] A.S. Kherbeet, H.A. Mohammed, K.M. Munisamy, B.H. Salman, The effect of step height of microscale backward-facing step on mixed convection nanofluid flow and heat transfer characteristics, Int. J. Heat Mass Transf. 68 (2014) 554–566, https://doi.org/10.1016/j.ijheatmasstransfer.2013.09.050.

[29] M.J. Esteve, P. Reulet, P. Millan, Flow field characterization within a rectangular cavity, in: 10th Int. Symp. Appl. Laser Tech. to Fluid Mech., Lisbon, Portugal, 2000.

[30] J. Sinha, K. Arora, Review of the flow-field analysis over cavities, Int. Conf. Infocom Technol. Unmanned Syst. (Trends Futur. Dir IEEE), 2017, pp. 870–876 10.1109/ICTUS.2017.8286128.

[31] A. Mushyam, J.M. Bergada, C. Navid Nayeri, A numerical investigation of laminar flow over a backward facing inclined step, Meccanica. 51 (2016) 1739–1762, https://doi.org/10.1007/s11012-015-0335-5.

[32] A. Singh, A. Paul, P. Ranjan, Investigation of reattachment length for a turbulent flow over a backward facing step for different step angle, Int. J. Eng. Sci. Technol. 3 (2011) 84–88, https://doi.org/10.4314/ijest.v3i2.68135.

[33] H.H. Choi, V.T. Nguyen, J. Nguyen, Numerical Investigation of Backward Facing Step Flow over Various Step Angles, Procedia Eng. 154 (2016) 420–425, https://doi.org/10.1016/j.proeng.2016.07.508.
[34] H.R. Bravo, Y.-H. Zheng, Turbulent Flow over Step with Rounded Edges: Experimental and Numerical Study, J. Hydraul. Eng. 126 (2000) 82–85, https://doi.org/10.1061/(ASCE)0733-9429(2000)126:1(82).
[35] M.G. Carvalho, F. Durst, J.C.F. Pereira, Predictions and measurements of laminar flow over two-dimensional obstacles, Appl. Math. Model. 11 (1987) 23–34, https://doi.org/10.1016/0307-904X(87)90181-8.